Check for updates

blood advances

American Society of Hematology
2021 L Street NW, Suite 900,
Washington, DC 20036
Phone: 202-776-0544 | Fax 202-776-0545
bloodadvances@hematology.org

The E592K variant of SF3B1 creates unique RNA missplicing and associates with high-risk MDS without ring sideroblasts

Tracking no: ADV-2023-011260R3

In Young Choi (Johns Hopkins University, United States) Jonathan Ling (Johns Hopkins University School of Medicine, United States) Jian Zhang (Columbia University, United States) Eric Helmenstine (The Johns Hopkins Sidney Kimmel Comprehensive Cancer Center, United States) Wencke Walter (Munich Leukemia Laboratory, Germany) Panagiotis Tsakiroglou (The Johns Hopkins Sidney Kimmel Comprehensive Cancer Center, United States) Riley Bergman (Vanderbilt University, United States) Céline Philippe (Barts Cancer Institute, Queen Mary University of London, United Kingdom) James Manley (Columbia University, United States) Kevin Rouault-Pierre (Queen Mary University of London, United Kingdom) Bing Li (Institute of Hematology and Blood Diseases Hospital, Chinese Academy of Medical Sciences, China) Daniel Wiseman (The University of Manchester, United Kingdom) Kiran Batta (The University of Manchester, United Kingdom) Madhu Ouseph (Weill Cornell Medicine, United States) Elsa Bernard (Gustave Roussy, France) Benjamin Dubner (The Johns Hopkins Sidney Kimmel Comprehensive Cancer Center, United States) Xiao Li (Shanghai Jiao Tong University Affiliated Sixth People's Hospital, China) Torsten Haferlach (MLL Munich Leukemia Laboratory, Germany) Anna Koget (Allegheny Health Network Cancer Institute, United States) Salman Fazal (Allegheny Health Network Cancer Institute, United States) Tania Jain (Johns Hopkins University, United States) Christopher Gocke (Johns Hopkins Medical Institutions, United States) Amy DeZern (The Sidney Kimmel Comprehensive Cancer Center at Johns Hopkins, United States) William Dalton (The Johns Hopkins Sidney Kimmel Comprehensive Cancer Center, United States)

Abstract:
Among the most common genetic alterations in the myelodysplastic syndromes (MDS) are mutations in the spliceosome gene SF3B1. Such mutations induce specific RNA missplicing events, directly promote ring sideroblast (RS) formation, and generally associate with more favorable prognosis. However, not all SF3B1 mutations are the same, and little is known about how distinct hotspots influence disease. Here we report that the E592K variant of SF3B1 associates with high-risk disease features in MDS, including a lack of RS, increased myeloblasts, a distinct co-mutation pattern, and a lack of the favorable survival seen with other SF3B1 mutations. Moreover, compared to other hotspot SF3B1 mutations, E592K induces a unique RNA missplicing pattern, retains an interaction with the splicing factor SUGP1, and preserves normal RNA splicing of the sideroblastic anemia genes TMEM14C and ABCB7. These data have implications for our understanding of the functional diversity of spliceosome mutations, as well as the pathobiology, classification, prognosis, and management of SF3B1-mutant MDS.

Conflict of interest: COI declared - see note

COI notes: TJ: Institutional research support from CTI Biopharma, Kartos therapeutics, Incyte, Bristol Myers Squibb; Advisory board participation with Bristol Myers Squibb, Incyte, Abbvie, CTI, Kite, Cogent Biosciences, Blueprint Medicine, Telios pharma, Protagonist therapeutics, Galapagos, Tscan therapeutics, Karyopharm, Morphosys. SF has consulted for and received honoraria from Blueprint, CTI, Sobi, Bristol Myers Squibb, Abbvie, Gilead, GSK, Incyte, Janssen, Jazz, Karyopharm, Novartis, PharmaEssentia, Sanofi, Servier, Stemline, Taiho, and Takeda The authors declare no other competing interests.

Preprint server: Yes; Research Square https://assets.researchsquare.com/files/rs-2802265/v1/1247f669-b590-4818-8da2-254fd35e7e45.pdf?c=1687267926

Downloaded from http://ashpublications.net/bloodadvances/article-pdf/doi/10.1182/bloodadvances.2023011260/2225913/bloodadvances.2023011260.pdf by guest on 02 June 2024

Author contributions and disclosures: AED and WBD conceived the study. IYC, JPL, JZ, EH, JLM, KRP, AED, and WBD designed research. IYC, JPL, JZ, EH, CP, and WBD performed experiments. JLM, KRP, and WBD supervised experiments. IYC, WW, RB, CP, BL, DHW, KB, MO, EB, XL, TF, SF, CDG, TJ, AED, and WBD collected data. IYC, JPL, JZ, WW, JLM, KRP, AED, and WBD analyzed data. IYC, JPL, JZ, KRP, and WBD prepared figures. IYC and WBD wrote the manuscript. All authors critically reviewed and approved the final version of the manuscript.

Non-author contributions and disclosures: No;

Agreement to Share Publication-Related Data and Data Sharing Statement: Raw FASTQ files are deposited at the NCBI Sequence Read Archive (SRA) under accession number PRJNA1107944

Clinical trial registration information (if any):

Downloaded from http://ashpublications.net/bloodadvances/article-pdf/doi/10.1182/bloodadvances.2023011260/2225913/bloodadvances.2023011260.pdf by guest on 02 June 2024

The E592K variant of SF3B1 creates unique RNA missplicing and associates with high-risk MDS without ring sideroblasts

In Young Choi[1], Jonathan P. Ling[2,3,4], Jian Zhang[5], Eric Helmenstine[1], Wencke Walter[6], Panagiotis Tsakiroglou[1], Riley E. Bergman[7], Celine Phillipe[8], James L. Manley[5], Kevin Rouault-Pierre[8], Bing Li[9,10], Daniel H. Wiseman[11,12], Kiran Batta[11,12], Madhu Ouseph[13], Elsa Bernard[14,15], Benjamin Dubner[1], Xiao Li[16], Torsten Haferlach[6], Anna Koget[17], Salman Fazal[17], Tania Jain[1], Christopher D. Gocke[1,2], Amy E. DeZern[1], and W. Brian Dalton[1].

[1]The Sidney Kimmel Comprehensive Cancer Center, Johns Hopkins University School of Medicine, Baltimore, MD 21205, USA.

[2]Departments of Pathology, Johns Hopkins University School of Medicine, Baltimore, MD 21205, USA.

[3]Solomon H. Snyder Department of Neuroscience, Johns Hopkins University School of Medicine, Baltimore, MD 21205, USA.

[4]Kavli Neuroscience Discovery Institute, Johns Hopkins University, Baltimore, MD 21218, USA.

[5]Department of Biological Sciences, Columbia University, New York, NY 10027, USA.

[6]MLL Munich Leukemia Laboratory, Max-Lebsche-Platz 31, 81377, Munich, Germany.

[7]Division of Hematology, Oncology, Department of Medicine, Vanderbilt University Medical Center and The Vanderbilt-Ingram Cancer Center, Nashville, TN, USA.

[8]Barts Cancer Institute, Queen Mary University of London, London, UK.

[9]State Key Laboratory of Experimental Hematology, National Clinical Research Center for Blood Diseases, Haihe Laboratory of Cell Ecosystem, Institute of Hematology and Blood Diseases Hospital, Chinese Academy of Medical Sciences & Peking Union Medical College, Tianjin, China.

Downloaded from http://ashpublications.net/bloodadvances/article-pdf/doi/10.1182/bloodadvances.2023011260/2225913/bloodadvances.2023011260.pdf by guest on 02 June 2024

[10]MDS and MPN Centre, Institute of Hematology and Blood Diseases Hospital, Chinese Academy of Medical Sciences & Peking Union Medical College, Tianjin, China.

[11]Epigenetics of Haematopoiesis Laboratory, Division of Cancer Sciences, The University of Manchester, Manchester, UK.

[12]Department of Haematology, The Christie NHS Foundation Trust, Manchester, UK.

[13]Division of Pathology & Laboratory Medicine, Weill Cornell Medicine, New York, New York, USA.

[14]Computational Oncology Service, Department of Epidemiology & Biostatistics, Memorial Sloan Kettering Cancer Center, New York, NY, USA.

[15]Center for Hematologic Malignancies, Memorial Sloan Kettering Cancer Center, New York, NY, USA.

[16]Department of Hematology, Shanghai Jiao, Tong University Affiliated Sixth People's Hospital, Shanghai 200233, China.

[17]Allegheny Health Network Cancer Institute, Pittsburgh, Pennsylvania, USA.

Corresponding author
William Brian Dalton
The Johns Hopkins Sidney Kimmel Comprehensive Cancer Center
Cancer Research Building Room 2M07
1650 Orleans St.
Baltimore, Maryland 21231
United States
(410)6146173
wdalton2@jhmi.edu

Data Availability Statement

Raw FASTQ files are deposited at the NCBI Sequence Read Archive (SRA) under accession number PRJNA1107944

Downloaded from http://ashpublications.net/bloodadvances/article-pdf/doi/10.1182/bloodadvances.2023011260/2225913/bloodadvances.2023011260.pdf by guest on 02 June 2024

Downloaded from http://ashpublications.net/bloodadvances/article-pdf/doi/10.1182/bloodadvances.2023011260/2225913/bloodadvances.2023011260.pdf by guest on 02 June 2024

Abstract

Among the most common genetic alterations in the myelodysplastic syndromes (MDS) are mutations in the spliceosome gene *SF3B1*. Such mutations induce specific RNA missplicing events, directly promote ring sideroblast (RS) formation, and generally associate with more favorable prognosis. However, not all *SF3B1* mutations are the same, and little is known about how distinct hotspots influence disease. Here we report that the E592K variant of *SF3B1* associates with high-risk disease features in MDS, including a lack of RS, increased myeloblasts, a distinct co-mutation pattern, and a lack of the favorable survival seen with other SF3B1 mutations. Moreover, compared to other hotspot SF3B1 mutations, E592K induces a unique RNA missplicing pattern, retains an interaction with the splicing factor *SUGP1*, and preserves normal RNA splicing of the sideroblastic anemia genes *TMEM14C* and ABCB7. These data have implications for our understanding of the functional diversity of spliceosome mutations, as well as the pathobiology, classification, prognosis, and management of *SF3B1*-mutant MDS.

Key Point 1: The E592K variant of SF3B1 induces unique RNA missplicing that is nonoverlapping with other MDS-associated variants

Key Point 2: E592K is associated with elevated blasts, lack of ring sideroblasts, and decreased survival

Downloaded from http://ashpublications.net/bloodadvances/article-pdf/doi/10.1182/bloodadvances.2023011260/2225913/bloodadvances.2023011260.pdf by guest on 02 June 2024

Introduction

SF3B1 is the most mutated spliceosome gene in MDS, with an overall frequency of >30%[1]. The mutations are primarily missense substitutions that induce neomorphic RNA missplicing in thousands of junctions, which in turn alter expression of hundreds of genes in diverse pathways[2]. Mutant *SF3B1*-induced missplicing has been implicated in many MDS phenotypes, including dysfunctional iron metabolism, formation of ring sideroblasts, activation of innate immune signaling, and promotion of hematopoietic stem cell self-renewal[3–8]. *SF3B1* mutations also contain prognostic value in MDS, generally associating with more indolent disease progression, though with important exceptions[9–12]. In MDS treatment, mutant *SF3B1* has been a direct or indirect target of many investigational therapies. Thus, *SF3B1* mutations figure prominently in the research of—and clinical practice for—many MDS patients.

Not well understood is whether—and how—distinct *SF3B1* mutation hotspots differentially affect disease features and/or the RNA missplicing events that drive them. Previously, in an analysis of patients and cell models with *SF3B1* exon 14-15 mutations, we found that the K666N variant was enriched in high-risk MDS and produced an asymmetrical lack of missplicing events that are induced by K700E and H662Q mutations[13]. Here we report the results of extending this approach to a larger cohort of patients that included exon 13-16 mutations and additional cell models. This analysis revealed a striking distinctiveness in biological and clinical features of the *SF3B1* mutation E592K, which has implications for the understanding and management of *SF3B1*-mutant MDS.

Materials/Subjects and Methods

Patients

The mutation-agnostic acquisition of *SF3B1* mutations from cases of MDS and AML came from 3 sources: (1) the Sidney Kimmel Cancer Center at Johns Hopkins, the Vanderbilt-

Downloaded from http://ashpublications.net/bloodadvances/article-pdf/doi/10.1182/bloodadvances.2023011260/2225913/bloodadvances.2023011260.pdf by guest on 02 June 2024

Ingram Cancer Center, the MDS and MPN Centre at the Chinese Academy of Medical Sciences, the Munich Leukemia Laboratory, and the Allegheny Health Network Cancer Institute; (2) the Project Genie database[14], and (3) extraction from 86 publications (supplemental References). Use of all deidentified patient data were approved by the Institutional Review Boards at the respective institutions. Additional details are in supplemental methods.

Cells

HEK293T, TF1, and K562 cells were obtained from the ATCC. BC1 hiPSCs were a gift from Zack Wang (Johns Hopkins). HEK293T cells were grown in DMEM/10% FBS, K562 in RPMI/20% FBS, TF1 cells in RPMI/20% FBS with 2 ng/mL GM-CSF, and BC1 in mTeSR Plus. STR authentication and mycoplasma testing were done upon receipt and routinely thereafter, with last testing 2/2022.

hiPSC knockins

Knockins were generated using a two-step targeting process similar to the CORRECT method of Paquet et al[15]. Additional details are in supplemental methods.

Transcriptome analysis

Total RNA isolation, cDNA synthesis, isoform-competitive endpoint PCR, and isoform-independent quantitative PCR with SYBR Green were performed as described[13,16]. All primer sequences are listed in supplemental Table 1. RNA-seq libraries from TF1 clones were constructed using TruSeq Stranded Total RNA Library Prep. Sequencing was performed on a NovaSeq S1 flowcell. Reads were aligned using STAR[17]. Splicing analysis was performed using ASCOT algorithms and gene expression using featureCounts[18,19]. Additional details are in supplemental methods.

Downloaded from http://ashpublications.net/bloodadvances/article-pdf/doi/10.1182/bloodadvances.2023011260/2225913/bloodadvances.2023011260.pdf by guest on 02 June 2024

Affinity Purification of *SF3B1*-Associated Proteins

A small-scale protocol was applied to both HEK293T and TF1 cells as previously described, except that for TF1, 10 million cells were used and proteins were eluted with 30 µL (5 µg/µL) 3X FLAG peptide because cells had only one affinity tag (FLAG) attached to SF3B1[20].

Western Blotting

Immunoblotting of proteins following affinity purification of SF3B1 in HEK293T and TF1 cells was performed as previously described[20]. Additional details are in supplemental methods.

Use of deidentified patient data were approved by the Institutional Review Boards at the respective institutions.

Results

Combining patient data from five institutions, publicly available databases, and published literature, we established a dataset of 3,330 patients with *SF3B1*-mutant MDS or AML in which exons 13 through 16 had been sequenced. We first determined how *SF3B1* mutations partitioned into WHO 2016 classifications, as these data were available for virtually all patients. This distribution showed several asymmetries (Figure 1 and supplemental Figure 1). Consistent with our previous report[13], the frequency of K666N was progressively higher in disease types of increasing risk: only 2.1% (28/1360) in MDS-RS vs 9.3% (23/248) in MDS-SLD/MLD, 17.7% (48/272) in MDS-EB, and 25.0% (137/548) in AML (p-value compared to MDS-RS = 2.7e-6, 1.5e-19, and 1.6e-51, respectively). With the inclusion of cases in which exon 13 had been sequenced, a disproportionately low frequency in MDS-RS was also revealed for a variant from this exon, E592K: only 0.07% (1/1360) in MDS-RS vs 3.6% in (9/248) in MDS-SLD/MLD, 3.3% (9/272) in MDS-EB, and 2.4% (13/548) in AML (p-value compared to MDS-RS = 3.8e-7, 7.6e-7, and 8.4e-7, respectively). Conversely, E622D was decreased in higher-risk disease: 7.0%

Downloaded from http://ashpublications.net/bloodadvances/article-pdf/doi/10.1182/bloodadvances.2023011260/2225913/bloodadvances.2023011260.pdf by guest on 02 June 2024

(95/1360) in MDS-RS vs 2.8% (7/248) in MDS-SLD/MLD ($p<0.05$), 0.4% (1/272) in MDS-EB ($p<0.0001$), and 0.5% (3/548) in AML (p-value compared to MDS-RS = 1.0e-2, 6.2e-7, and 2.4e-11, respectively). K666R also decreased: 5.5% (75/1360) in MDS-RS vs 1.2% (3/248) in MDS-SLD/MLD, 1.1% (3/272) in MDS-EB, and 2.2% (12/548) in AML (p-value compared to MDS-RS = 1.9e-3, 8.5e-4, and 1.0e-3, respectively). These data confirm and extend the scope of asymmetrical partitioning of distinct *SF3B1* hotspots in MDS disease subtypes.

We next examined RNA splicing events produced by those *SF3B1* mutations with the most significant asymmetric partitioning. We expressed FLAG-tagged codon-optimized constructs with the E592K, E622D, K666N, and K666R mutations in HEK293 cells, along with wild type *SF3B1* and the dominant K700E mutation. For additional comparison, we expressed variants from solid tumors that are rare (R625H, K741N) or absent (E902K) in myeloid malignancies[21]. These transfections produced a comparable level of endogenous and exogenous *SF3B1* protein (Figure 2). Upon expression of most hotspots, we observed missplicing in junctions known to be affected by *SF3B1* mutations, including *SLTM*, *ZDHHC16* and *MAP3K7* (Figure 2)[2,6]. This included MDS mutations K700E, E622D, K666R, and K666N but also solid tumor hotspots R625H and K741N, the last of which produced lower magnitude missplicing as recently reported in the context of uveal melanoma[22]. In contrast, these junctions were not misspliced by E902K, which showed its own unique missplicing pattern as was noted in TCGA E902K bladder cancer samples (supplemental Figure 2)[21]. We also found that two other mutant *SF3B1*-associated junctions, in *DLST* and *UQCC1*, were misspliced to high magnitude by most mutations but were unaffected by K666N, confirming that the pattern of missplicing by K666N is different from that of other MDS/AML-associated hotspots[13,23]. Notably, this pattern occurred with K666N, but not K666R, demonstrating these variants are not functionally equivalent even though they affect the same starting amino acid, a phenomenon also observed with variants in the yeast homologue of *SF3B1*[24]. Finally, conspicuously absent

Downloaded from http://ashpublications.net/bloodadvances/article-pdf/doi/10.1182/bloodadvances.2023011260/2225913/bloodadvances.2023011260.pdf by guest on 02 June 2024

was any missplicing of these events by E592K. Coupled with its near-absence in MDS-RS, this distinct missplicing pattern motivated us to investigate E592K further.

We characterized the clinical features of E592K patients in more detail. The hotspot-agnostic collection of all patients with exon 13-16 sequencing had produced 40 cases of E592K, comprising 1.2% (40/3300) of SF3B1-mutant MDS/AML in our dataset and 0.25% (8/3323) of all MDS in the IPSS-M cohort[10]. By specifically seeking out additional cases from multiple institutions, we gathered a total of 51 patients with E592K-mutated myeloid neoplasms, 45 of which were MDS or AML (supplemental Table 2). This expanded E592K cohort also showed asymmetry in 2016 WHO classifications, and these patients had higher IPSS-M scores, IPSS-R scores, and lower platelets than cases with exon 14-16 mutations (Figure 3A-C and supplemental Figure 3A). Hemoglobin and WBC were not significantly different (supplemental Figure 3B-C). E592K cases also had a notable lack of RS (supplemental Figure 3D), with only one instance of low-blast E592K MDS reporting any RS, at 8%, therein being the only E592K patient to meet WHO 2016 criteria for MDS-RS (>5% RS if *SF3B1* mutation present). By contrast, for low-blast MDS with exon 14-16 mutations in which exact RS percentages were available, the average was 37%, consistent with the known pathological and mechanistic links between mutant *SF3B1* and RS in MDS (Figure 3D)[5,25]. E592K MDS and AML also had a notable co-mutation profile (Figure 4 and supplemental Figures 4-7). Like exon 14-16 mutations, E592K co-occurred rarely with mutations in other splicing factors (SRSF2, U2AF1, ZRSR2), a pattern consistent with pathogenicity for spliceosome mutations. However, a striking distinction was the nearly ubiquitous co-mutation of ASXL1 (85%) in E592K MDS, compared to only 12% in exon 14-16 MDS (p=1.1e-16, q=2.4E-15). High ASXL1 co-mutation characterized both low and high blast E592K cases, suggesting this relationship occurs early in disease evolution (supplemental Figure 4-6). E592K MDS patients also had increased co-mutations of RUNX1 (35% vs 8%) and STAG2 (38% vs 4%) (p=2.1e-10 and 5.0e-8, q=2.2e-9 and 3.5e-7, respectively). Additionally, there was a noteworthy trend towards mutual exclusivity between

Downloaded from http://ashpublications.net/bloodadvances/article-pdf/doi/10.1182/bloodadvances.2023011260/2225913/bloodadvances.2023011260.pdf by guest on 02 June 2024

E592K and DNMT3A co-mutations (4%) in MDS, despite DNMT3A being the 2nd most commonly co-mutated gene (24%) in exon 14-16 MDS (p=0.017 but q = 0.074). In fact, the one DNMT3A mutation in E592K MDS was a VAF of 2.3% in a sample in which the VAFs for E592K and ASXL1 mutations were 20%, raising the possibility that the DNMT3A mutation was in a separate clone with wild type *SF3B1*. When all MDS and AML cases were considered together, the mutual exclusivity between E592K and DNMT3A mutations was significant (p=1.8e-3, q=8.8e-3, supplemental Figure 8). Finally, both overall survival and leukemia-free survival were markedly shorter in E592K MDS patients (Figure 3E and supplemental Figure 3E). Binary stratification into IPSS-M higher (score >0) or lower (score <0) categories showed that while outcomes were similarly poor for E592K and exon 14-16 patients in the higher group, E592K had significantly worse survival in the lower group (Figure 3F-G and supplemental Figure 3F-G). Analogous stratification using the IPSS-R yielded similar results (Supplemental Figure 8D-E). For additional context, we compared survival of our dataset to non-SF3B1-mutant patients from the cohort that trained the IPSS-M (supplemental Figure 8). Like E592K, non-SF3B1-mutant MDS had lower survival than exon 14-16, although binary stratification by the IPSS-M—and to a lesser extent the IPSS-R—separated the lower and higher risk non-SF3B1-mutant patients better than E592K. Taken together, these data demonstrate that SF3B1-mutant MDS patients with E592K have distinct and high-risk clinical features.

Because our initial splicing analysis merely showed the absence of known *SF3B1*-mutant events in E592K cells, we next sought missplicing events specifically induced by this variant. To do so, we stably expressed the WT, K700E, and E592K mutations through lentiviral delivery in TF1 cells, isolated multiple independent clones for each genotype, and performed RNA-seq to quantify percent spliced in (PSI) values for all splice junctions (Figure 5A). K700E produced a characteristic pattern of increased expression of junctions using alternative 3' acceptors, with high magnitude missplicing of genes like *MAP3K7* and *ZDHCC16*, as expected.

Downloaded from http://ashpublications.net/bloodadvances/article-pdf/doi/10.1182/bloodadvances.2023011260/2225913/bloodadvances.2023011260.pdf by guest on 02 June 2024

In contrast, the E592K mutation produced a fundamentally different pattern of missplicing, with its affected genes nonoverlapping with those misspliced by K700E, and vice-versa. Western blotting showed that exogenous FLAG-tagged *SF3B1* was equal or less than the endogenous *SF3B1* form, not overexpressed above it (Figure 5B). We then validated several missplicing events with endpoint and quantitative PCR assays. For K700E-specific junctions, this included missplicing of *ZDHHC16*, *TMEM14C*, and *ABCB7* (Figure 5B-C). For E592K-specific junctions, this included *RAVER2*, *CEP43*, *NUTM2A-AS1*, and *EZH2* (Figure 5D). Interestingly, the EZH2 missplicing event was an alternate acceptor in intron 12, creating a premature termination codon predicted to activate nonsense-mediated decay (Figure 5E). We further validated the hotspot specificity of these events in two other overexpression contexts: transiently-transfected HEK293T and stably-transduced K562 cells (supplemental Figure 9). To determine the effect of precisely heterozygous expression of these variants from their natural genetic elements, we also queried hotspot-specific missplicing in human induced pluripotent stem cells (hiPSCs) that we engineered with heterozygous knockins of K700E, E592K, and R702R (a SNP in the human population) (Figure 5E-F and supplemental Figure 10). In all cases, K700E- and E592K-dependent missplicing events were present and distinct. Of note, missplicing of *TMEM14C* and *ABCB7* were recently shown to drive ring sideroblast formation in iPSCs derived from *SF3B1*-mutant MDS[5]. Both genes were clearly misspliced by K700E, but not by E592K, consistent with the lack of sideroblastic anemia in E592K patients. Together, these data show that the E592K variant of *SF3B1* has a unique pattern of RNA missplicing.

In addition to shared RNA missplicing events, the most well-studied *SF3B1* hotspot mutations also share a specific biochemical defect: disruption of the interaction between *SF3B1* and *SUGP1*[20]. This disruption is not incidental to missplicing but directly mediates it; inactivation of *SUGP1* recapitulates *SF3B1*-mutant missplicing and overexpression of *SUGP1* partially rescues it[20]. We therefore asked whether E592K, with its nonoverlapping missplicing events, might preserve the interaction of *SF3B1* with *SUGP1*. Indeed, when His6-FLAG-*SF3B1* variants

Downloaded from http://ashpublications.net/bloodadvances/article-pdf/doi/10.1182/bloodadvances.2023011260/2225913/bloodadvances.2023011260.pdf by guest on 02 June 2024

were introduced into HEK293T cells and affinity purified using anti-DYKDDDDK (FLAG) antibody and cobalt beads, the association of His6-FLAG-*SF3B1* with endogenous *SUGP1* was disrupted by K700E but not by wild type or E592K *SF3B1* (Figure 6). We then asked whether E592K might instead disrupt the interaction between *SF3B1* and *PHF5A*, given that E592 is in HEAT repeat 3 at the interface with *PHF5A*[26]. However, this interaction was preserved by each His6-FLAG-SF3B1 variant (Figure 6). We also observed these effects in a second cell context, TF1 cells expressing FLAG-*SF3B1* variants (supplemental Figure 11). Together, these data indicate that, consistent with its induction of unique RNA missplicing events, the E592K variant does not participate in the disruption of the *SF3B1-SUGP1* interaction that drives the cryptic splicing of other *SF3B1* mutations.

Finally, we identified and analyzed RNA-seq from two patients with E592K mutation, compared to other *SF3B1* mutations, from the recent MLL cohort of spliceosome-mutant myeloid malignancy patients[27]. Inspection of the junctions validated in our cell models also demonstrated the same specificity of missplicing in these primary patient samples, when compared to other *SF3B1* mutations (Figure 7A). In addition, endpoint PCR validation of TMEM14C and RAVER2 from a third primary E592K sample at a separate institution demonstrated the same hotspot specificity of RNA missplicing (Figure 7B), validating the findings from our cell models.

Discussion

Here we show the E592K variant of *SF3B1* produces unique RNA missplicing and associates with high-risk MDS. These results have several implications. First, the distinctiveness of E592K informs the pathobiology of *SF3B1*-mutant MDS. Clough et al elegantly showed that RS are formed by TMEM14C and ABCB7 missplicing in MDS-derived iPSCs with the G742D variant of *SF3B1*[5]. These missplicing events have been seen with other hotspots, including K700E, which we corroborated here[2,28]. Cells with E592K, on the other hand, preserved canonical splicing of these genes, and cases of E592K MDS lacked RS. Other events

Downloaded from http://ashpublications.net/bloodadvances/article-pdf/doi/10.1182/bloodadvances.2023011260/2225913/bloodadvances.2023011260.pdf by guest on 02 June 2024

that have been implicated in *SF3B1*-mutant MDS pathobiology include innate immune activation by missplicing of MAP3K7 and IRAK4, enhanced self-renewal by MECOM missplicing, impaired erythropoiesis by COASY missplicing, and hepcidin suppression by ERFE missplicing; all these genes were also canonically spliced in E592K cells (supplemental Figure 12)[3,4,6–8]. A distinct E592K pathobiology is also suggested by its high co-occurrence with ASXL1/RUNX1/STAG2 mutations and mutual exclusivity with DNMT3A mutations, a starkly different pattern than that of other *SF3B1* hotspots. As with most co-mutation patterns in cancer, it is unclear whether these co-occurrences are driven by synergism or permissiveness—and whether the mutual exclusivity is driven by antagonism or redundancy. Interestingly, the same pattern of co-occurrence (ASXL1/RUNX1/STAG2) and mutual exclusivity (DNMT3A) occurs with loss-of-function EZH2 mutations in MDS (supplemental Figure 13)[10,14]. It is therefore intriguing that E592K missplicing produced a frameshifted EZH2 transcript in our studies here, and it is tempting to speculate this may create 'mutant EZH2-ness' in E592K cells, an area for future investigation. If so, mutual exclusivity due to redundancy might be expected between mutant EZH2 and E592K. While there were indeed no EZH2 mutations in the 51 E592K patients here, the low overall frequency (4%) of EZH2 in *SF3B1*-mutant myeloid malignancies means a larger cohort would be needed for significance testing of this particular pair. Nonetheless, the distinctiveness of E592K here shows that certain MDS phenotypes associated with *SF3B1* mutation, including sideroblastic anemia, are not inevitable pathobiological outcomes of RNA missplicing by all *SF3B1* variants.

Second, there are implications for MDS classification. Recently, both the International Consensus Classification (ICC) and the 5th edition of the World Health Organization (WHO) classification of myeloid neoplasms created nosologic entities for *SF3B1*-mutant MDS[29,30]. These are based on the International Working Group (IWG) findings that *SF3B1* mutation, low blasts, and lack of certain co-occurring genetic aberrations defined an indolent MDS with a shared pathobiology of idiosyncratic RNA missplicing that was more homogeneous than the MDS-RS classification[31]. This was due in part to exclusion of *SF3B1*-unmutated MDS-RS which

Downloaded from http://ashpublications.net/bloodadvances/article-pdf/doi/10.1182/bloodadvances.2023011260/2225913/bloodadvances.2023011260.pdf by guest on 02 June 2024

had greater myeloid/megakaryocyte dysplasia, more TP53 co-mutations, and poorer outcomes. Both the ICC and WHO criteria require *SF3B1* mutation, low blasts, cytopenias, dysplasia, and lack of multi-hit TP53/del(5q)/-7/complex cytogenetics; the ICC also requires *SF3B1* VAF>10% and lack of RUNX1/del(7q)/abn3q26.2 and the WHO allows for >15% RS to substitute for *SF3B1* mutation. As we have seen here, E592K patients do not fit these groups: they have unique RNA missplicing, higher blasts, lack of RS, increased RUNX1 mutations, and poorer prognosis. While E592K is, overall, an infrequent mutation, these differences do suggest that E592K could be considered an additional exclusion criterion for these entities. They also suggest consideration of specific hotspot mutations in future classification efforts. If so, this would be the precise mutation, not just the affected amino acid, as we demonstrated different patterns of disease partitioning and missplicing between K666R and K666N.

Third, our data have implications for prognostication of E592K patients. Along with low blasts, shallow cytopenias, and certain cytogenetic abnormalities such as del(11q), *SF3B1* mutations have been consistently associated with better MDS outcomes in multiple independent datasets[1,9–12]. Accordingly, new MDS prognosis scoring tools incorporating mutational data have generally weighted *SF3B1* mutations favorably, although there is important context-dependence that overrides this favorability, such as increased blasts and aberrations such as del(5q), RUNX1 mutation, and others[10–12]. However, given the much larger patient cohorts that would be required, prognostication tools do not yet separately weight the myriad individual variants of mutated genes (*SF3B1* or otherwise) into their scores. In our cohort, the group defined by higher IPSS-M risk categories included E592K and exon 14-16 patients with similarly poor outcomes, while the group composed of lower risk categories captured patients with better outcomes for exon 14-16, but not E592K, disease (Figure 3E-G). While the numbers of E592K patients in these groups is still modest overall, these data nonetheless suggest caution in regarding any E592K patients as lower risk. For example, patients #9 and #1 progressed from MDS to AML at 6 and 9 months, respectively, despite lower-risk scores from both the IPSS-M

Downloaded from http://ashpublications.net/bloodadvances/article-pdf/doi/10.1182/bloodadvances.2023011260/2225913/bloodadvances.2023011260.pdf by guest on 02 June 2024

and SEX-GSS (supplemental Figure 14). Again, with the caveat that E592K is uncommon and may represent a special case, our findings suggest consideration of incorporating specific hotspot mutations in future prognostication tools.

Fourth, these results have implications for investigational therapies that target the missplicing defects of SF3B1-mutant cells. Gene vector therapies that leverage missplicing to deploy therapeutic cargo against spliceosome-mutant cells are promising, but such vectors would need to be not only gene-specific (i.e. *SF3B1* vs *SRSF2*) but, in the case of E592K, hotspot-specific due to its nonoverlapping missplicing[32,33]. Antisense oligonucleotide therapy aimed at rescuing *BRD9* missplicing showed activity against *SF3B1*-mutant tumors in vivo, but such a therapy would not apply to E592K, which does not missplice *BRD9* (supplemental Figure 10)[34]. It is also possible that synthetic lethality approaches of further disrupting the spliceosome itself in SF3B1-mutant cells could affect E592K cells differently[35].

Finally, these findings add to our understanding of the functional diversity of spliceosome mutations. After these mutations were first discovered as conspicuously enriched in myeloid neoplasms in a mutually exclusive manner, efforts have sought unifying downstream functional effects that might explain this occurrence pattern[36]. This has revealed shared phenotypes, such as convergent disruption of certain pathways or genes (e.g. mutant SRSF2 missplices EZH2 but at a different junction than we observed here for SF3B1 E592K), creation of genotoxic R-loops, and sensitization to further disruption of the spliceosome[6,35,37–41]. At the same time, bulk and then single-cell analyses have shown that spliceosome mutations are not always mutually exclusive, with multiple mutations sometimes selected for in the same cells[23]. This indicates that different spliceosome mutations can confer different, even complementary, advantages to cancer cells, and the mutual exclusivity that does occur may be more from the splicing toxicity of combining certain mutations than from functional redundancy[23]. Consistent with this, studies have shown direct functional differences between spliceosome mutations: the missplicing events induced by mutations in different spliceosome genes (i.e. *SRSF2* vs *U2AF1*, etc) are

Downloaded from http://ashpublications.net/bloodadvances/article-pdf/doi/10.1182/bloodadvances.2023011260/2225913/bloodadvances.2023011260.pdf by guest on 02 June 2024

nonoverlapping, the two dominant hotspot mutations in *U2AF1* missplice different genes, and some less common *SRSF2* and *U2AF1* variants only partially or "dually" recapitulate the RNA missplicing of hotspot mutations[2,40,42–44]. For *SF3B1* mutations, their asymmetric partitioning among cancer types (i.e. K700E/H662Q in MDS, R625C/R625H in uveal melanoma, G642D in CLL, etc.) first suggested the mutations may have functional differences[36,45,46]. Later, Seiler et al noted different missplicing events in TCGA RNA-seq from bladder tumors with the E902K variant, events that we experimentally confirmed here[21]. For other *SF3B1* hotspots, studies have described differences of degree in RNA missplicing events, including K700E vs R625C/R625H in primary samples, R625H vs K741Q vs others in isogenic cells, and K666N vs K700E/H662Q in primary samples and isogenic cells[13,22,23,47]. To these we add E592K, whose missplicing events are differences of kind, nonoverlapping with those of other MDS-associated hotspots. We also find distinct biochemistry for E592K, with preservation of the interaction between *SUGP1* and *SF3B1*, and future work should include screening for altered interactions between E592K and other spliceosome proteins. While it remains possible that the important underlying oncogenic effects of E592K are phenotypes still shared with other *SF3B1* hotspots, the distinctiveness of E592K suggests to us that different *SF3B1* variants can promote different kinds of leukemia by inducing different RNA missplicing events. Because these differences can impact our understanding and management of patients with myeloid neoplasms, additional studies of differences between other spliceosome variants are warranted.

Acknowledgements

This work was supported by grants from the NIH (HL159306), Edward P. Evans Foundation, Leukemia & Lymphoma Society, Maryland Stem Cell Research Fund, Gabrielle's Angel Foundation for Cancer Research, Emerson Collective, and AbbVie (to WBD); NIH R35 GM118136 (to JLM); Lady Tata Memorial Trust (3218) and the Barts Charity (G-002167) (to CP and KR). DHW is supported by an Advanced Clinician Scientist Fellowship from Cancer

Downloaded from http://ashpublications.net/bloodadvances/article-pdf/doi/10.1182/bloodadvances.2023011260/2225913/bloodadvances.2023011260.pdf by guest on 02 June 2024

Research UK, a grant from the The Oglesby Charitable Trust and the University of Manchester's Sybil Mary Pilkington Leukaemia Research Fellowship.

Author Contributions

AED and WBD conceived the study. IYC, JPL, JZ, EH, JLM, KRP, AED, and WBD designed research. IYC, JPL, JZ, EH, PT, CP, BD, and WBD performed experiments. JLM, KRP, and WBD supervised experiments. IYC, WW, RB, CP, BL, DHW, KB, MO, EB, XL, TH, AK, SF, CDG, TJ, AED, and WBD collected data. IYC, JPL, JZ, WW, JLM, KRP, AED, and WBD analyzed data. IYC, JPL, JZ, KRP, and WBD prepared figures. IYC and WBD wrote the manuscript. All authors critically reviewed and approved the final version of the manuscript.

Competing Interests

TJ: Institutional research support from CTI Biopharma, Kartos therapeutics, Incyte, Bristol Myers Squibb; Advisory board participation with Bristol Myers Squibb, Incyte, Abbvie, CTI, Kite, Cogent Biosciences, Blueprint Medicine, Telios pharma, Protagonist therapeutics, Galapagos, Tscan therapeutics, Karyopharm, Morphosys. SF has consulted for and received honoraria from Blueprint, CTI, Sobi, Bristol Myers Squibb, Abbvie, Gilead, GSK, Incyte, Janssen, Jazz, Karyopharm, Novartis, PharmaEssentia, Sanofi, Servier, Stemline, Taiho, and Takeda

The authors declare no other competing interests.

References

1. Haferlach T, Nagata Y, Grossmann V, et al. Landscape of genetic lesions in 944 patients with myelodysplastic syndromes. *Leukemia*. 2014;28(2):241–7.

2. Darman RB, Seiler M, Agrawal AA, et al. Cancer-Associated SF3B1 Hotspot Mutations Induce Cryptic 3′ Splice Site Selection through Use of a Different Branch Point. *Cell Reports*. 2015;13(5):1033–1045.

3. Bondu S, Alary A-S, Lefèvre C, et al. A variant erythroferrone disrupts iron homeostasis in SF3B1-mutated myelodysplastic syndrome. *Sci Transl Med*. 2019;11(500):eaav5467.

4. Mian SA, Philippe C, Maniati E, et al. Vitamin B5 and succinyl-CoA improve ineffective erythropoiesis in SF3B1-mutated myelodysplasia. *Sci Transl Med*. 2023;15(685):eabn5135.

Downloaded from http://ashpublications.net/bloodadvances/article-pdf/doi/10.1182/bloodadvances.2023011260/2225913/bloodadvances.2023011260.pdf by guest on 02 June 2024

5. Clough CA, Pangallo J, Sarchi M, et al. Coordinated mis-splicing of TMEM14C and ABCB7 causes ring sideroblast formation in SF3B1-mutant myelodysplastic syndrome. *Blood*. 2021;139(13):2038–2049.

6. Lee SC-W, North K, Kim E, et al. Synthetic Lethal and Convergent Biological Effects of Cancer-Associated Spliceosomal Gene Mutations. *Cancer Cell*. 2018;34(2):225-241.e8.

7. Choudhary GS, Pellagatti A, Agianian B, et al. Activation of targetable inflammatory immune signaling is seen in myelodysplastic syndromes with SF3B1 mutations. *Elife*. 2022;11:e78136.

8. Tanaka A, Nakano TA, Nomura M, et al. Aberrant EVI1 splicing contributes to EVI1-rearranged leukemia. *Blood*. 2022;140(8):875–888.

9. Malcovati L, Papaemmanuil E, Bowen DT, et al. Clinical significance of SF3B1 mutations in myelodysplastic syndromes and myelodysplastic/myeloproliferative neoplasms. *Blood*. 2011;118(24):6239–6246.

10. Bernard E, Tuechler H, Greenberg PL, et al. Molecular International Prognostic Scoring System for Myelodysplastic Syndromes. *Nejm Évid*. 2022;1(7):.

11. Bersanelli M, Travaglino E, Meggendorfer M, et al. Classification and Personalized Prognostic Assessment on the Basis of Clinical and Genomic Features in Myelodysplastic Syndromes. *J Clin Oncol*. 2021;39(11):1223–1233.

12. Nazha A, Komrokji R, Meggendorfer M, et al. Personalized Prediction Model to Risk Stratify Patients With Myelodysplastic Syndromes. *J Clin Oncol*. 2021;39(33):3737–3746.

13. Dalton WB, Helmenstine E, Pieterse L, et al. The K666N mutation in SF3B1 is associated with increased progression of MDS and distinct RNA splicing. *Blood Adv*. 2020;4(7):1192–1196.

14. Consortium TAPG, André F, Arnedos M, et al. AACR Project GENIE: Powering Precision Medicine through an International Consortium. *Cancer Discov*. 2017;7(8):818–831.

15. Paquet D, Kwart D, Chen A, et al. Efficient introduction of specific homozygous and heterozygous mutations using CRISPR/Cas9. *Nature*. 2016;533(7601):125–9.

16. Dalton WB, Helmenstine E, Walsh N, et al. Hotspot SF3B1 mutations induce metabolic reprogramming and vulnerability to serine deprivation. *J Clin Invest*. 2019;129(11):4708–4723.

17. Dobin A, Davis CA, Schlesinger F, et al. STAR: ultrafast universal RNA-seq aligner. *Bioinformatics*. 2013;29(1):15–21.

18. Ling JP, Wilks C, Charles R, et al. ASCOT identifies key regulators of neuronal subtype-specific splicing. *Nat Commun*. 2020;11(1):137.

19. Liao Y, Smyth GK, Shi W. featureCounts: an efficient general purpose program for assigning sequence reads to genomic features. *Bioinformatics*. 2014;30(7):923–930.

20. Zhang J, Ali AM, Lieu YK, et al. Disease-Causing Mutations in SF3B1 Alter Splicing by Disrupting Interaction with SUGP1. *Mol Cell*. 2019;76(1):82-95.e7.

Downloaded from http://ashpublications.net/bloodadvances/article-pdf/doi/10.1182/bloodadvances.2023011260/2225913/bloodadvances.2023011260.pdf by guest on 02 June 2024

21. Seiler M, Peng S, Agrawal AA, et al. Somatic Mutational Landscape of Splicing Factor Genes and Their Functional Consequences across 33 Cancer Types. *Cell Reports*. 2018;23(1):282-296.e4.

22. Canbezdi C, Tarin M, Houy A, et al. Functional and conformational impact of cancer-associated SF3B1 mutations depends on the position and the charge of amino acid substitution. *Comput Struct Biotechnology J*. 2021;19:1361–1370.

23. Taylor J, Mi X, North K, et al. Single-cell genomics reveals the genetic and molecular bases for escape from mutational epistasis in myeloid neoplasms. *Blood*. 2020;136(13):1477–1486.

24. Carrocci TJ, Zoerner DM, Paulson JC, Hoskins AA. SF3b1 mutations associated with myelodysplastic syndromes alter the fidelity of branchsite selection in yeast. *Nucleic Acids Res*. 2017;gkw1349.

25. Papaemmanuil E, Cazzola M, Boultwood J, et al. Somatic SF3B1 Mutation in Myelodysplasia with Ring Sideroblasts. *New Engl J Medicine*. 2011;365(15):1384–1395.

26. Cretu C, Schmitzová J, Ponce-Salvatierra A, et al. Molecular Architecture of SF3b and Structural Consequences of Its Cancer-Related Mutations. *Molecular cell*. 2016;64(2):307–319.

27. Hershberger CE, Moyer DC, Adema V, et al. Complex landscape of alternative splicing in myeloid neoplasms. *Leukemia*. 2021;35(4):1108–1120.

28. Conte S, Katayama S, Vesterlund L, et al. Aberrant splicing of genes involved in haemoglobin synthesis and impaired terminal erythroid maturation in SF3B1 mutated refractory anaemia with ring sideroblasts. *Brit J Haematol*. 2015;171(4):478–490.

29. Arber DA, Orazi A, Hasserjian RP, et al. International Consensus Classification of Myeloid Neoplasms and Acute Leukemia: Integrating Morphological, Clinical, and Genomic Data. *Blood*. 2022;

30. Khoury JD, Solary E, Abla O, et al. The 5th edition of the World Health Organization Classification of Haematolymphoid Tumours: Myeloid and Histiocytic/Dendritic Neoplasms. *Leukemia*. 2022;36(7):1703–1719.

31. Malcovati L, Stevenson K, Papaemmanuil E, et al. SF3B1-mutant MDS as a distinct disease subtype: a proposal from the International Working Group for the Prognosis of MDS. *Blood*. 2020;136(2):157–170.

32. North K, Benbarche S, Liu B, et al. Synthetic introns enable splicing factor mutation-dependent targeting of cancer cells. *Nat Biotechnol*. 2022;1–11.

33. Ling JP, Bygrave AM, Santiago CP, et al. Cell-specific regulation of gene expression using splicing-dependent frameshifting. *Nat Commun*. 2022;13(1):5773.

34. Inoue D, Chew G-L, Liu B, et al. Spliceosomal disruption of the non-canonical BAF complex in cancer. *Nature*. 2019;574(7778):432–436.

35. Lee SC, Dvinge H, Kim E, et al. Modulation of splicing catalysis for therapeutic targeting of leukemia with mutations in genes encoding spliceosomal proteins. *Nature medicine*. 2016;22(6):672–8.

Downloaded from http://ashpublications.net/bloodadvances/article-pdf/doi/10.1182/bloodadvances.2023011260/2225913/bloodadvances.2023011260.pdf by guest on 02 June 2024

36. Yoshida K, Sanada M, Shiraishi Y, et al. Frequent pathway mutations of splicing machinery in myelodysplasia. *Nature*. 2011;478(7367):64–9.

37. Chen L, Chen J-Y, Huang Y-J, et al. The Augmented R-Loop Is a Unifying Mechanism for Myelodysplastic Syndromes Induced by High-Risk Splicing Factor Mutations. *Mol Cell*. 2018;69(3):412-425.e6.

38. Pellagatti A, Armstrong RN, Steeples V, et al. Impact of spliceosome mutations on RNA splicing in myelodysplasia: dysregulated genes/pathways and clinical associations. *Blood*. 2018;132(12):1225–1240.

39. Shiozawa Y, Malcovati L, Gallì A, et al. Aberrant splicing and defective mRNA production induced by somatic spliceosome mutations in myelodysplasia. *Nat Commun*. 2018;9(1):3649.

40. Kim E, Ilagan JO, Liang Y, et al. SRSF2 Mutations Contribute to Myelodysplasia by Mutant-Specific Effects on Exon Recognition. *Cancer cell*. 2015;27(5):617–30.

41. Pangallo J, Kiladjian J-J, Cassinat B, et al. Rare and private spliceosomal gene mutations drive partial, complete, and dual phenocopies of hotspot alterations. *Blood*. 2020;

42. Zhang J, Lieu YK, Ali AM, et al. Disease-associated mutation in SRSF2 misregulates splicing by altering RNA-binding affinities. *Proc National Acad Sci*. 2015;112(34):E4726–E4734.

43. Madan V, Kanojia D, Li J, et al. Aberrant splicing of U12-type introns is the hallmark of ZRSR2 mutant myelodysplastic syndrome. *Nat Commun*. 2015;6(1):6042.

44. Ilagan JO, Ramakrishnan A, Hayes B, et al. U2AF1 mutations alter splice site recognition in hematological malignancies. *Genome Research*. 2015;25(1):14–26.

45. Harbour WJ, Roberson ED, Anbunathan H, et al. Recurrent mutations at codon 625 of the splicing factor SF3B1 in uveal melanoma. *Nature Genetics*. 2013;45(2):133.

46. Rossi D, Bruscaggin A, Spina V, et al. Mutations of the SF3B1 splicing factor in chronic lymphocytic leukemia: association with progression and fludarabine-refractoriness. *Blood*. 2011;118(26):6904–8.

47. Liu Z, Yoshimi A, Wang J, et al. Mutations in the RNA Splicing Factor SF3B1 Promote Tumorigenesis through MYC Stabilization. *Cancer Discov*. 2020;10(6):806–821.

Downloaded from http://ashpublications.net/bloodadvances/article-pdf/doi/10.1182/bloodadvances.2023011260/2225913/bloodadvances.2023011260.pdf by guest on 02 June 2024

Figure 1. Distribution of exon 13-16 SF3B1 mutations within WHO 2016 classifications of MDS and AML. Amino acid positions are shown along the x axis, and individual variants are counted along the y axis according to the legend above the graphs. RS = ring sideroblasts. SLD/MLD = single-lineage dysplasia/multi-lineage dysplasia. EB = excess blasts.

Figure 2. Asymmetric RNA missplicing by distinct SF3B1 mutation hotspots. HEK293T cells were transfected with constructs expressing FLAG-SF3B1 variants. Top row is Western blotting with anti-SF3B1 antibody, showing FLAG-SF3B1 and endogenous SF3B1 at similar levels. Endpoint PCR used isoform-competitive primers, with arrows for canonical (blue), cryptic (red), and heteroduplex (green) forms. Cryptic vs canonical UQCC1 was quantified as a ratio between two separate isoform-specific qPCRs.

Figure 3. Clinical parameters of MDS patients with the E592K variant of SF3B1. Compared to cases with exon 14-16 mutations, patients with E592K have A) higher fractions of MDS-SLD/MLD, MDS-EB, and AML, B) higher IPSS-M, C) lower platelets, D) nearly-absent ring sideroblasts (RS), and E) lower overall survival which is retained in F) lower IPSS-M score groups. Outcomes are similarly poor for E592K and exon 14-16 patients in G) higher IPSS-M score groups..

Figure 4. Co-mutation landscape of MDS with E592K or exon 14-16 SF3B1 mutations. All cases of SF3B1-mutant MDS that sequenced at least the 24 additional genes shown were included. Fisher's exact test p-values and Benjamini linear multiple testing q-values for FDR<0.05 were as follows: ****ASXL1 = 1.13E-16 and 2.37E-15; ****RUNX1 = 2.06E-10 and 2.16E-09; ****STAG2 = 5.03E-08 and 3.52E-07; *NRAS = 4.61E-03 and 2.42E-02.

Downloaded from http://ashpublications.net/bloodadvances/article-pdf/doi/10.1182/bloodadvances.2023011260/2225913/bloodadvances.2023011260.pdf by guest on 02 June 2024

Figure 5. E592K induces unique RNA missplicing events. TF1 cells transduced with different SF3B1 variants were analyzed by RNA-seq, with A) highest-scoring ΔPSIs shown. B) Western blot with anti-SF3B1 antibody. C) Endpoint PCR/qPCR validation of K700E-specific missplicing events. D) Validation of E592K-specific events. E) RNA-seq reads from TF1 cells showing the cryptic event in EZH2. PTC = premature termination codon. F) Orthogonal validation of missplicing in heterozygous SF3B1 knockin hiPSCs.

Figure 6. The E592K variant preserves association of SF3B1 with SUGP1. HEK293T cells were transfected with His6-FLAG-SF3B1 variants and subjected to affinity purification with anti-DYKDDDDK (FLAG) antibody. A) Silver-stained protein gel, with arrow pointing to the size of SUGP1, which is decreased in K700E but not E592K eluate. B) Western blot showing decreased SUGP1 in K700E, but not E592K, eluate. PHF5A is present with all SF3B1 variants. C) Reprobing with anti-SF3B1 shows native and His6-FLAG-tagged protein levels. KD = kilodaltons. M = marker. Vec = vector only. W = wild type SF3B1. K = K700E. E = E592K.

Figure 7. E592K exhibits unique RNA missplicing in primary MDS samples. RNA-seq read distribution in the MLL cohort shows that E592K exhibits A) canonical TMEM14C and ABCB7 missplicing, and B) cryptic RAVER2, NUTM2B-AS1, and EZH2 missplicing. C) Distinct TMEM14C and RAVER2 missplicing was validated in marrow CD34+ cells from an independent patient by endpoint PCR.

Downloaded from http://ashpublications.net/bloodadvances/article-pdf/doi/10.1182/bloodadvances.2023011260/2225913/bloodadvances.2023011260.pdf by guest on 02 June 2024

Figure 1

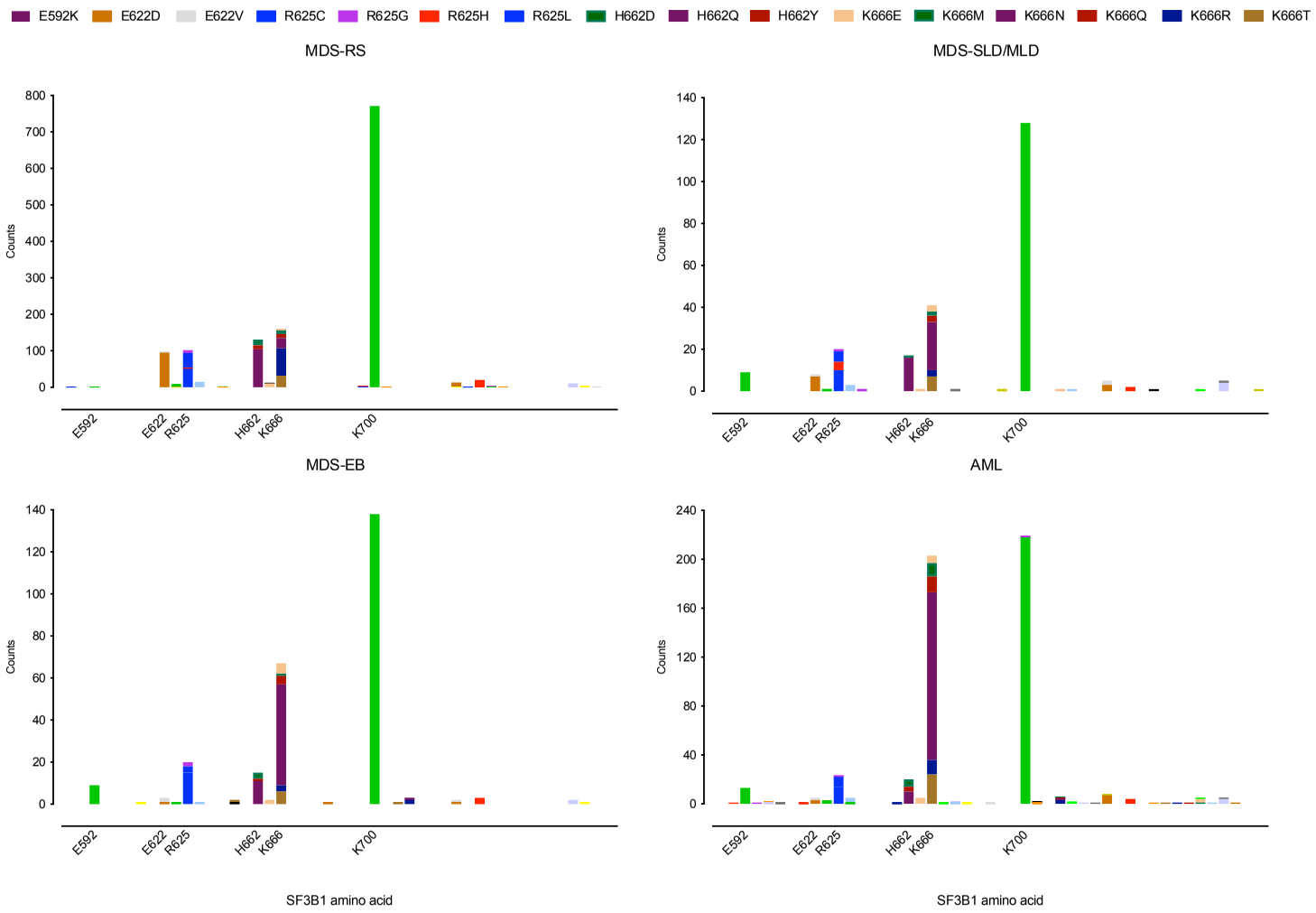

Figure 1. Distribution of exon 13-16 SF3B1 mutations within WHO 2016 classifications of MDS and AML. Amino acid positions are shown along the x axis, and individual variants are counted along the y axis according to the legend above the graphs. RS = ring sideroblasts. SLD/MLD = single-lineage dysplasia/multi-lineage dysplasia. EB = excess blasts.

Downloaded from http://ashpublications.net/bloodadvances/article-pdf/doi/10.1182/bloodadvances.2023011260/2225913/bloodadvances.2023011260.pdf by guest on 02 June 2024

Figure 2

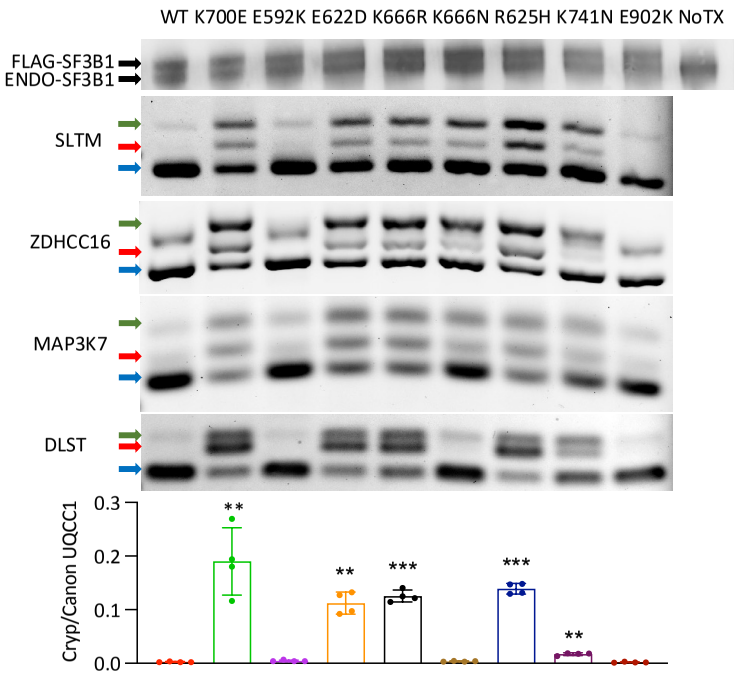

Figure 2. Asymmetric RNA missplicing by distinct SF3B1 mutation hotspots. HEK293T cells were transfected with constructs expressing FLAG-SF3B1 variants. Top row is Western blotting with anti-SF3B1 antibody, showing FLAG-SF3B1 and endogenous SF3B1 at similar levels. Endpoint PCR used isoform-competitive primers, with arrows for canonical (blue), cryptic (red), and heteroduplex (green) forms. Cryptic vs canonical UQCC1 was quantified as a ratio between two separate isoform-specific qPCRs.

Downloaded from http://ashpublications.net/bloodadvances/article-pdf/doi/10.1182/bloodadvances.2023011260/2225913/bloodadvances.2023011260.pdf by guest on 02 June 2024

Figure 3

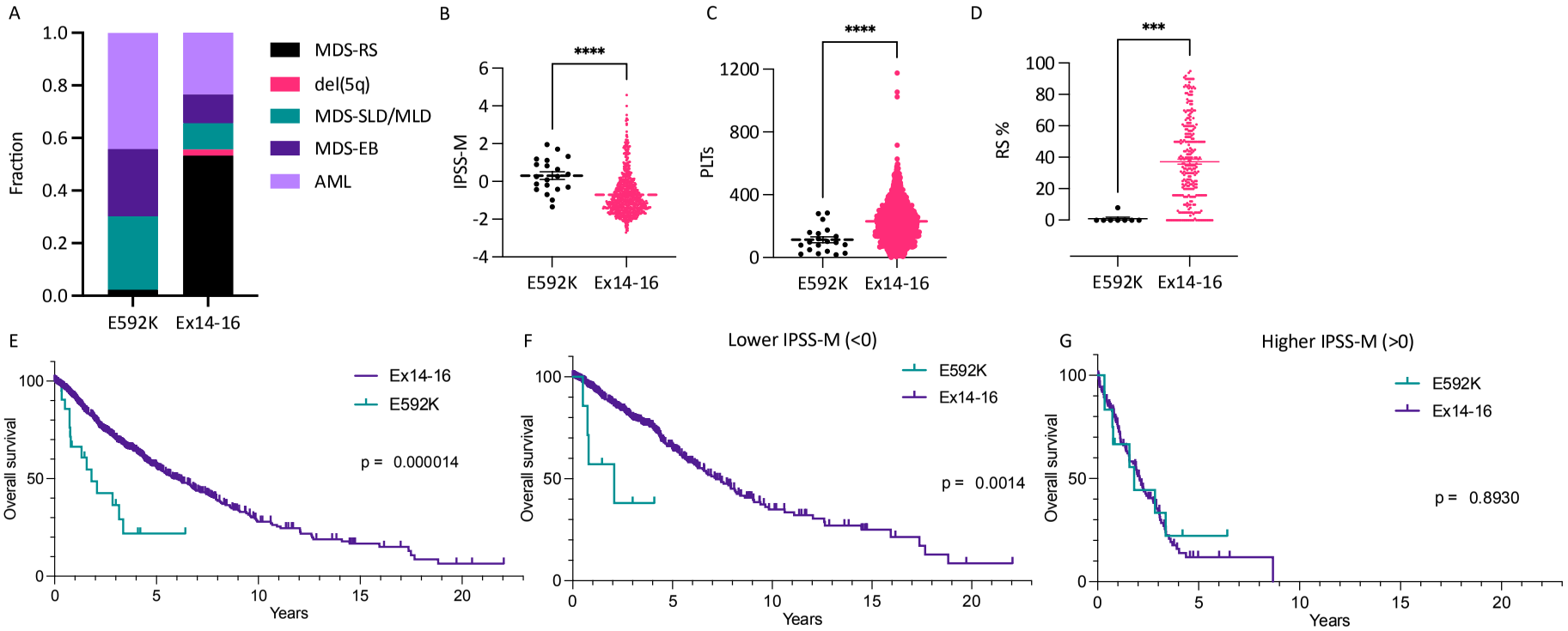

Figure 3. Clinical parameters of MDS patients with the E592K variant of SF3B1. Compared to cases with exon 14-16 mutations, patients with E592K have A) higher fractions of MDS-SLD/MLD, MDS-EB, and AML, B) higher IPSS-M, C) lower platelets, D) nearly-absent ring sideroblasts (RS), and E) lower overall survival which is retained in F) lower IPSS-M score groups. Outcomes are similarly poor for E592K and exon 14-16 patients in G) higher IPSS-M score groups..

Downloaded from http://ashpublications.net/bloodadvances/article-pdf/doi/10.1182/bloodadvances.2023011260/2225913/bloodadvances.2023011260.pdf by guest on 02 June 2024

Figure 4

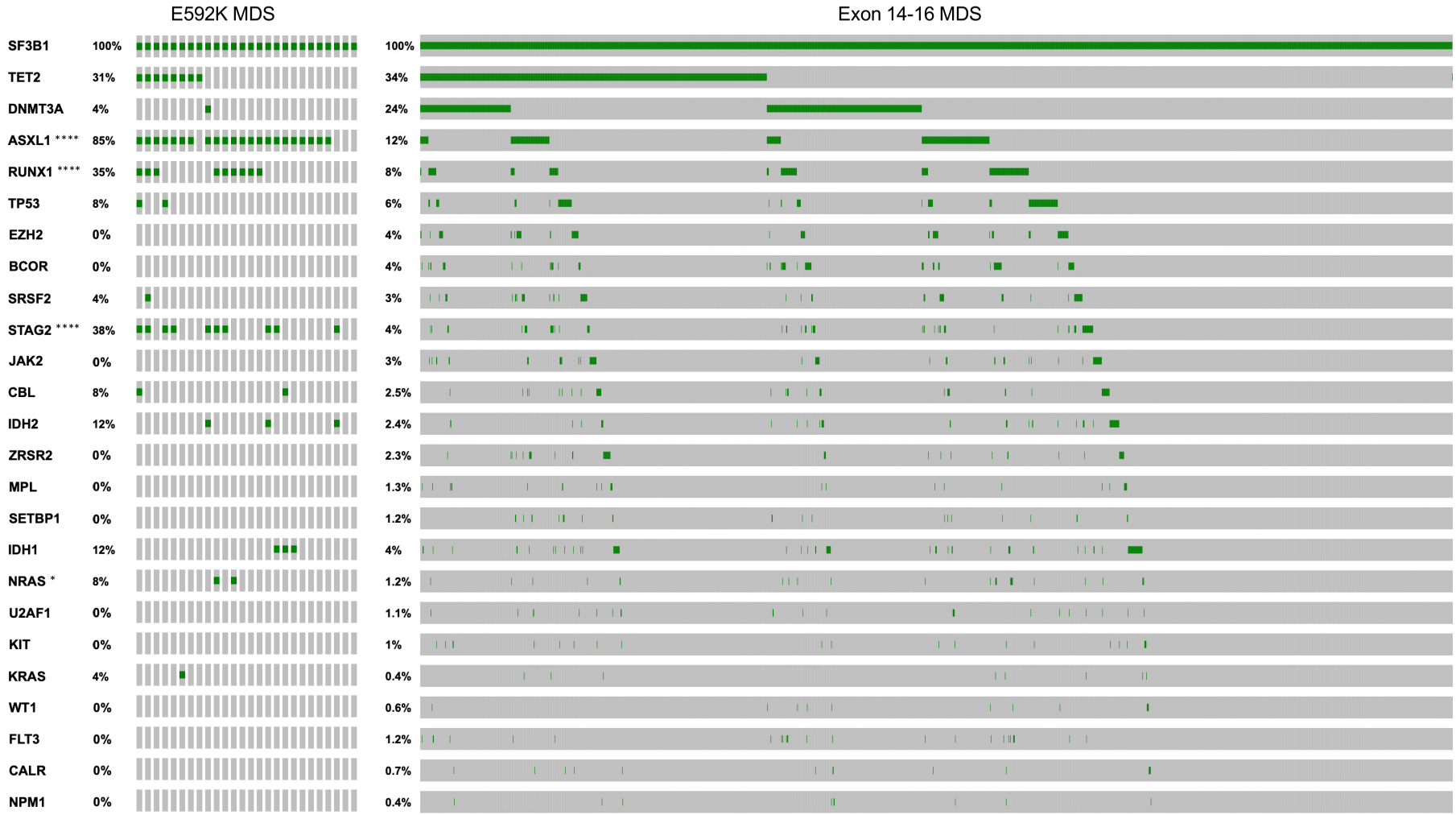

Figure 4. Co-mutation landscape of MDS with E592K or exon 14-16 SF3B1 mutations. All cases of SF3B1-mutant MDS that sequenced at least the 24 additional genes shown were included. Fisher's exact test p-values and Benjamini linear multiple testing q-values for FDR<0.05 were as follows: ****ASXL1 = 1.13E-16 and 2.37E-15; ****RUNX1 = 2.06E-10 and 2.16E-09; ****STAG2 = 5.03E-08 and 3.52E-07; *NRAS = 4.61E-03 and 2.42E-02.

Downloaded from http://ashpublications.net/bloodadvances/article-pdf/doi/10.1182/bloodadvances.2023011260/2225913/bloodadvances.2023011260.pdf by guest on 02 June 2024

Figure 5

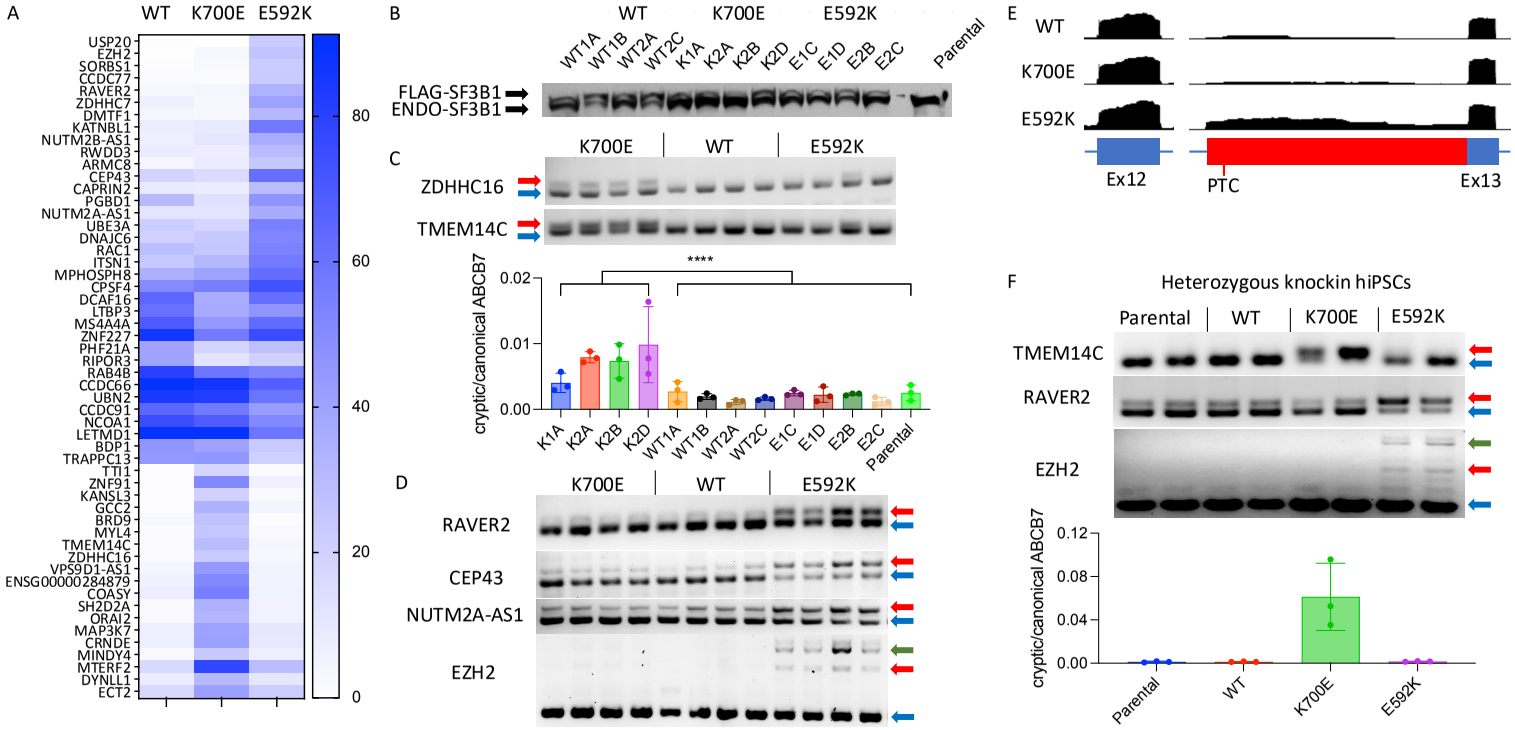

Figure 5. E592K induces unique RNA missplicing events. TF1 cells transduced with different SF3B1 variants were analyzed by RNA-seq, with A) highest-scoring ΔPSIs shown. B) Western blot with anti-SF3B1 antibody. C) Endpoint PCR/qPCR validation of K700E-specific missplicing events. D) Validation of E592K-specific events. E) RNA-seq reads from TF1 cells showing the cryptic event in EZH2. PTC = premature termination codon. F) Orthogonal validation of missplicing in heterozygous SF3B1 knockin hiPSCs.

Downloaded from http://ashpublications.net/bloodadvances/article-pdf/doi/10.1182/bloodadvances.2023011260/2225913/bloodadvances.2023011260.pdf by guest on 02 June 2024

Figure 6

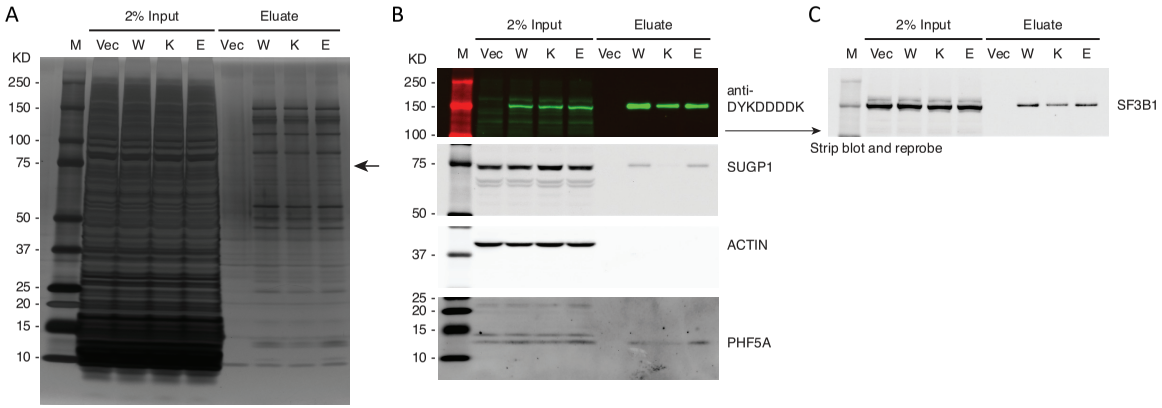

Figure 6. The E592K variant preserves association of SF3B1 with SUGP1. HEK293T cells were transfected with His6-FLAG-SF3B1 variants and subjected to affinity purification with anti-DYKDDDDK (FLAG) antibody. A) Silver-stained protein gel, with arrow pointing to the size of SUGP1, which is decreased in K700E but not E592K eluate. B) Western blot showing decreased SUGP1 in K700E, but not E592K, eluate. PHF5A is present with all SF3B1 variants. C) Reprobing with anti-SF3B1 shows native and His6-FLAG-tagged protein levels. KD = kilodaltons. M = marker. Vec = vector only. W = wild type SF3B1. K = K700E. E = E592K.

Downloaded from http://ashpublications.net/bloodadvances/article-pdf/doi/10.1182/bloodadvances.2023011260/2225913/bloodadvances.2023011260.pdf by guest on 02 June 2024

Figure 7

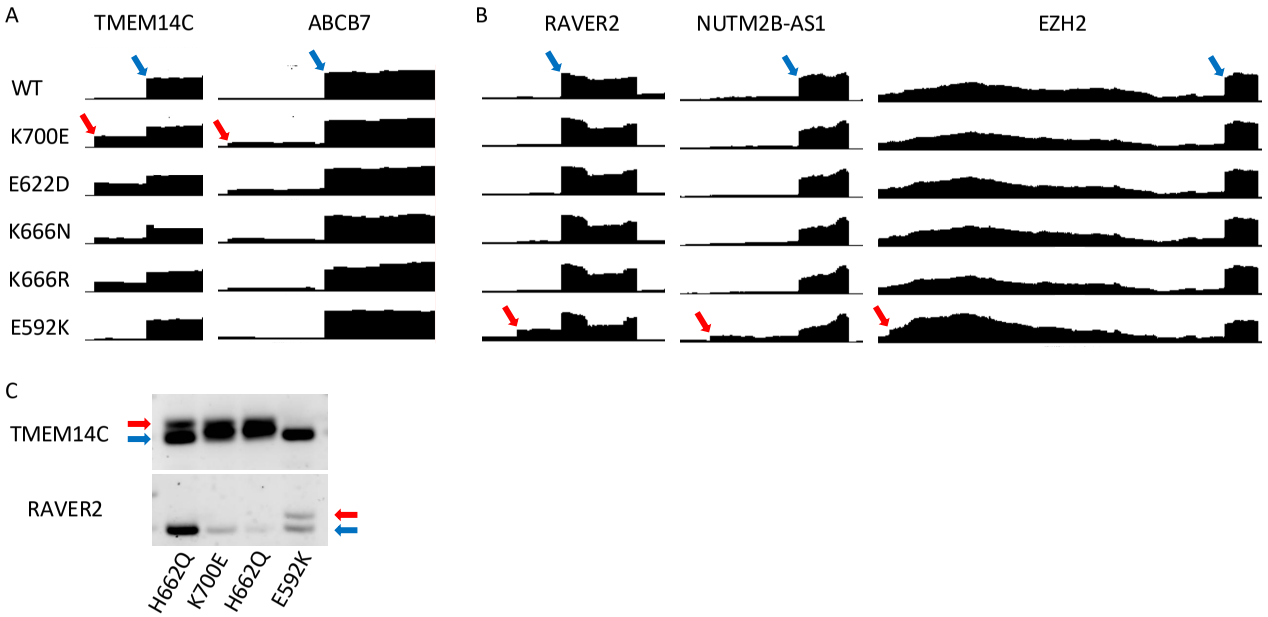

Figure 7. E592K exhibits unique RNA missplicing in primary MDS samples. RNA-seq read distribution in the MLL cohort shows that E592K exhibits A) canonical TMEM14C and ABCB7 missplicing, and B) cryptic RAVER2, NUTM2B-AS1, and EZH2 missplicing. C) Distinct TMEM14C and RAVER2 missplicing was validated in marrow CD34+ cells from an independent patient by endpoint PCR.

Downloaded from http://ashpublications.net/bloodadvances/article-pdf/doi/10.1182/bloodadvances.2023011260/2225913/bloodadvances.2023011260.pdf by guest on 02 June 2024